arXiv:hep-ph/9710237v2 6 Oct 1997

KEK Preprint 97-160
KEK-TH- 544
February 1, 2008

Enhancement of Loop Induced $H^{\pm}W^{\mp}Z^0$ Vertex in Two Higgs-doublet Model

Shinya Kanemura [1]

Theory Group, KEK,
Tsukuba, Ibaraki 305, Japan

Abstract

The non-decoupling effects of heavy Higgs bosons as well as fermions on the loop-induced $H^{\pm}W^{\mp}Z^0$ vertex are discussed in the general two Higgs doublet model. The decay width of the process $H^+ \to W^+Z^0$ is calculated at one-loop level and the possibility of its enhancement is explored both analytically and numerically. We find that the novel enhancement of the decay width can be realized by the Higgs non-decoupling effects with large mass-splitting between the charged Higgs boson and the CP-odd one. This is due to the large breakdown of the custodial $SU(2)_V$ invariance in the Higgs sector. The branching ratio can amount to $10^{-2} \sim 10^{-1}$ for $m_{H^{\pm}} = 300$ GeV within the constraint from the present experimental data. Hence this mode may be detectable at LHC or future e^+e^- linear colliders.

Key Words: Tow Higgs Doublet Model, Non-Decoupling Effects, Charged Higgs Boson.

[1]e-mail: kanemu@theory.kek.jp

1 Introduction

The standard model (SM) of the electroweak interaction has been tested by a lot of experiments and any substantial deviation from the data from the precision experiments such as at LEP and SLC [1] has not been found so far [2]. In spite of the success of SM, the symmetry breaking sector (Higgs sector) remains unknown. The Higgs sector is expected to be probed at LEP II [3], LHC [4] and future e^+e^- linear colliders (LC's) [5]. Although the minimal Higgs sector with only one Higgs doublet is consistent with the available experimental data, the Higgs sector may be favored to have rather a little more complicated structures from the various theoretical viewpoint [6]. One of the simplest but rich extensions of the minimal Higgs sector is the two Higgs doublet model (THDM). There are a lot of motivations for THDM such as the minimal supersymmetric standard model (MSSM), additional CP violating phases, and a solution of the strong CP problem.

The charged Higgs boson $H^\pm$ is one of the new particle contents in such the extended Higgs sectors and its exploration is a quite important task of the future experiments at LHC and LC's. If $H^\pm$ is relatively light ($< m_W$), it may be detected at LEP II. If $H^\pm$ has the mass of the intermediate scale ($m_W < m_{H^\pm} < m_t + m_b$), $H^\pm$ would be detected at future colliders such as LHC or LC through the decay modes $H^\pm \to \tau\nu$ and cs. Alternatively if $m_{H^\pm}$ is large enough to allow $H^\pm \to tb$ kinematically, it seems to be difficult to detect it because of the large QCD background. The heavy $H^\pm$ is, in fact, favored by the results of the $b \to s\gamma$ measurement in THDM with Type II Yukawa couplings [7] (There are narrow loopholes for this constraint in MSSM [8].). In such cases, we have to investigate the possibility of the alternative modes with the branching ratio enough to yield substantial events to probe $H^\pm$. The possible modes for such the purpose may be $H^\pm \to \tau\nu$, $h^0W^\pm$, $W^\pm Z^0$ and $W^\pm\gamma$. Unfortunately, it has been known that the latter two modes (namely, decays into a gauge boson pair) disappear at tree level in general multi Higgs-doublet models including THDM. This property is quite different from the case of (CP-even) neutral Higgs bosons. The absence of the tree $H^\pm W^\mp\gamma$ coupling comes from the current conservation of $U(1)_{\rm em}$. On the other hand, tree $H^\pm W^\mp Z^0$ coupling is absent because of the isospin symmetry of the kinetic term of the Higgs sector [9]. Since both these

characteristics are, in general, broken at one-loop level through effects from other sectors, these vertices are induced at loop level. Hence the question of how large the vertex can be enhanced by loop effects occurs. In fact, the estimations of the loop-induced decay widths for $H^\pm \to W^\pm Z^0$ and $H^\pm \to W^\pm \gamma$ have been studied in part by several authors: Pomarol and Mendez [10] once have studied $H^+ \to W^+ Z^0$ in MSSM, and Capdequi Peyranere et al. [11] have calculated the fermion and sfermion non-decoupling effects on $H^+ \to W^+ Z^0$ and $H^+ \to W^+ \gamma$. In their works, it has been pointed out that while the loop-induced $H^\pm W^\mp \gamma$ vertex is much small, the loop-induced $H^\pm W^\mp Z^0$ vertex can be largely enhanced by the mass effects of *super heavy* fermions. It, however, seems to be difficult to consider such the heavy fermions in the present situation that the top-quark has already been discovered at ~ 175 GeV [12] and that the fourth generation of fermions has been almost excluded by the S-parameter constraint [2, 13]. Hence the substantial enhancement of the vertices seems no longer to be possible in the framework of MSSM, in which the non-decoupling effects on the vertex are essentially only due to heavy fermions. Apart from MSSM, there are some exotic Higgs models with more complicated Higgs multiplets (for example, triplets) which have $H^\pm W^\mp Z^0$ coupling at tree level [14]. Therefore the decay mode $H^+ \to W^+ Z^0$ has often been considered as a clear signature for these exotic Higgs sectors.

Here occurs another question of how about the general THDM but MSSM. In MSSM, the Higgs mass-effects are very small because of their decoupling property and the fermion effects are dominant. On the other hand, there can be non-decoupling effects of heavy Higgs bosons in THDM in general. In such the model, whether the loop induced $H^\pm W^\mp Z^0$ vertex can be substantially enhanced by the Higgs mass-effects or not is a non-trivial and also very interesting problem. In the previous works [10, 11, 15], these effects have not been considered at all. The purpose of this paper is just to solve this problem.

In this paper, we discuss the loop induced $H^\pm W^\mp Z^0$ vertex in THDM. The possibility that this vertex can be largely enhanced by the non-decoupling effects of the heavy Higgs bosons is explored in detail. In the THDM Higgs sector, whether the heavy Higgs bosons are decoupled or not is rather model dependent. The heavy Higgs bosons, in general, receive their masses from both the vacuum expectation value and the (bare) non-zero soft-breaking parameter. If the contribution of the latter effect is relatively dominant,

the masses become approximately independent of the self-coupling constants and then the heavy Higgs bosons become decoupled [16]. The MSSM Higgs sector approximately corresponds to this case, in which all the quartic self-coupling constants are constrained to $\sim \mathcal{O}(g^2)$ and the Higgs bosons other than the lightest can become heavy only by the growing soft-breaking parameter. The effects of these heavy masses then should be suppressed by the decoupling theorem. This is one of the main reasons why the Higgs mass effects are less important than the fernion's ones in MSSM. Alternatively, if the heavy Higgs bosons are due to the large self-coupling constants, the masses naively become proportional to the coupling constants and then the non-decoupling effects of the Higgs bosons can be expected as well as those of the fermions [17, 18, 19]. Such the non-decoupling effects of the heavy Higgs bosons (for example, the effects of the heavier neutral boson H^0 or the CP-odd Higgs boson A^0) are of our central interest here.

From the naive power counting, the non-decoupling effects on the $H^{\pm}W^{\mp}Z^0$ vertex can be expected to include quadratic and logarithmic mass contributions at one loop level [11]. [2] However, by making the effective Lagrangian it is shown that these non-decoupling effects are completely canceled if the theory has the global custodial $SU(2)_V$ symmetry. There is the similar situation in the oblique corrections known as the screening theorem [20]. In THDM, the custodial symmetry in the Higgs sector is explicitly broken except for the case of the mass degeneracy between the $H^{\pm}$ and A^0 [21, 22]. Hence we expect that the large mass splitting leads to the quadratic Higgs mass effects to the vertex. Thus the conditions for large enhancement of the vertex by the heavy Higgs bosons are 1) the large Higgs masses coming from the larger contributions of the quartic coupling constants with keeping the soft-breaking parameter to be smaller, 2) the large explicit breaking of $SU(2)_V$ in the Higgs sector by large mass splitting between $H^{\pm}$ and A^0. We note that although THDM is indeed strongly constrained by the experimental results for the oblique corrections [23], there remains large allowed region for large mass splitting between $H^{\pm}$ and A^0 because of a lot of free parameters in the model [19].

[2] In the case of $H^{\pm}W^{\mp}\gamma$ vertex, only the logarithmic mass effects are possible because of the $U(1)_{em}$ current conservation [11]. Thus the non-decoupling effects cannot be so large. Hence we here consider $H^{\pm}W^{\mp}Z^0$ vertex only.

With the consideration above, we analyze the decay process $H^+ \to W^+Z^0$ at one loop level in THDM. The calculation is performed in the t'Hooft-Feynman gauge for the Higgs-Goldstone sector and gauge sector and in the unitary gauge for fermion loops. Since all the diagrams with a fermion-loop themselves construct a gauge invariant subset, we are free to use different gauge choices like above [11]. In addition to the conditions above, the vertex turns out to be much sensitive to the Higgs mixing angles. We find that the branching ratio $Br(H^+ \to W^+Z^0)$ at $m_{H^\pm} = 300$ GeV become larger than 10^{-2} if the mass splitting between H^+ and A^0 is larger than 200 GeV for $\tan\beta > 6 \sim 8$, where $\tan\beta = v_2/v_1$. The maximal value of $Br(H^+ \to W^+Z^0)$ can amount to near 10^{-1} for $\tan\beta > 20$ and very large m_{A^0} but within the allowed region from the tree-level unitarity bound [24]. Such the enhancement of the branching ratio ($10^{-2} \sim 10^{-1}$) may make it possible to detect the mode at LHC [4]. It is expected that more than a few dozen of the events ($H^\pm \to W^\pm Z^0 \to lll\nu$) are produced for the branching ratios of $\sim 10^{-2}$. As to the background (mainly from $u\bar{d} \to W^+Z^0$), it is likely such that the branching ratio of a few % would be required in order to see a signal [25]. Therefore in THDM the non-decoupling effects of Higgs bosons can induce a significant enhancement of the branching ratio and this process may become detectable at LHC. In the $SU(2)_V$ symmetric cases ($m_{A^0} \sim m_{H^\pm}$), the Higgs non-decoupling effects are canceled out and only the fermion and gauge boson contributions remain, so that the branching ratio becomes smaller than 10^{-4} for $\tan\beta > 1$. We also show that such the enhancement is reduced by taking account of the soft-breaking parameter to be large.

In Sec 2, we introduce THDM and discuss its decoupling and non-decoupling properties. Sec 3 is devoted to the qualitative study of the possibility of enhancement of the $H^\pm W^\mp Z^0$ vertex due to the non-decoupling effects. In Sec 4, the decay process $H^+ \to W^+Z^0$ is evaluated in THDM and the novel enhancement of the branching ratio is shown. In Sec 5, we summerize the results and discuss some phenomenological implication. The explicit results of the calculations are attached in Appendices.

2 The Model

In this paper, we discuss the non-decoupling effects of the additional heavy Higgs bosons as well as the fermions on the $H^{\pm}W^{\mp}Z^0$ vertex in the two Higgs doublet model (THDM). We here consider the model with a softly-broken discrete symmetry under $\Phi_1 \to \Phi_1$, $\Phi_2 \to -\Phi_2$ because there are too many parameters to be analyzed in the most general THDM. The discrete symmetry has often been imposed for natural avoiding of the flavor changing neutral current (FCNC) [26]. There are two types of Yukawa sector under the discrete symmetry according to the assignment of the charge of quarks, what we call, Type-I and Type-II in Ref [6]. We employ the Type-II coupling in our later calculation. The Higgs sector is defined by

$$\begin{aligned}\mathcal{L}^{int}_{\rm THDM} &= \mu_1^2\left|\Phi_1\right|^2 + \mu_2^2\left|\Phi_2\right|^2 + \left\{\mu_3^2\left(\Phi_1^\dagger\Phi_2\right) + \text{h.c.}\right\} \\ &\quad -\eta_1\left|\Phi_1\right|^4 - \eta_2\left|\Phi_2\right|^4 - \eta_3\left|\Phi_1\right|^2\left|\Phi_2\right|^2 \\ &\quad -\eta_4\left\{\left(\mathrm{Re}\Phi_1^\dagger\Phi_2\right)\right\}^2 - \eta_5\left\{\left(\mathrm{Im}\Phi_1^\dagger\Phi_2\right)\right\}^2. \end{aligned} \tag{1}$$

This potential covers the MSSM Higgs sector as a special case [6]. The soft-breaking parameter μ_3^2 is in general a complex quantity, which can give an additional CP violating source [27]. We here confine ourselves in the CP invariant world by assuming μ_3^2 to be real in order to reduce the number of parameters and also concentrate into extracting the essential contribution of the non-decoupling effects of the Higgs bosons.

The Higgs potential (1) has a global symmetry, that is, the custodial $SU(2)_V$ symmetry if η_5 is zero [21, 22]. To see this, it is convenient to rewrite RHS in (1) in terms of 2×2 matrices $\mathcal{M}_i = (i\tau_2\Phi_i^*, \Phi_i)$. All the terms except for the η_5-term can be rewritten as combinations of $\mathrm{tr}(\mathcal{M}_i^\dagger\mathcal{M}_j)$, $(i,j = 1 \text{ and/or } 2)$. Thereby it becomes clear that these terms are invariant under the transformation $\mathcal{M}_i \to g_L^\dagger\mathcal{M}_i g_R$, $(g_{L,R} \in SU(2)_{L,R}$, $SU(2)_L$ is the gauge symmetry of the weak interaction.). Hence, if η_5 is zero, there remains the global symmetry in the Higgs sector even after the gauge symmetry breaking; $SU(2)_L \otimes SU(2)_R \to SU(2)_V$ [28]. On the other hand, the η_5-term is rewritten as $\sim \eta_5\left\{\mathrm{tr}(\mathcal{M}_2\tau_3\mathcal{M}_1^\dagger)\right\}^2$. The η_5-term breaks $SU(2)_R$ and thus $SU(2)_V$ explicitly. Since the SM Higgs sector with one doublet is known to $SU(2)_V$ symmetric, the explicit breaking of $SU(2)_V$ in the Higgs sector leads to a new physics by itself. The custodial symmetry plays a crucial role in our

later discussion. [3]

The Higgs doublets both with $Y = 1/2$ are parametrized as

$$\Phi_i = \begin{pmatrix} w_i^+ \\ \frac{1}{\sqrt{2}}(h_i + v_i + iz_i) \end{pmatrix}, \ (i = 1, 2), \tag{2}$$

where the vacuum expectation values v_1 and v_2 are combined to give $v = \sqrt{v_1^2 + v_2^2} \sim$ 246GeV. The diagonalization of the mass matrices is performed by introducing two mixing angles α and β in the following way;

$$\begin{pmatrix} h_1 \\ h_2 \end{pmatrix} = R(\alpha) \begin{pmatrix} H^0 \\ h^0 \end{pmatrix}, \begin{pmatrix} w_1^\pm \\ w_2^\pm \end{pmatrix} = R(\beta) \begin{pmatrix} w^\pm \\ H^\pm \end{pmatrix}, \begin{pmatrix} z_1 \\ z_2 \end{pmatrix} = R(\beta) \begin{pmatrix} z^0 \\ A^0 \end{pmatrix},$$

where $R(\theta)$ is the usual rotation matrix of angle θ. After diagonalization with setting $\tan\beta = v_2/v_1$, the two mass-eigenstates $w^\pm$ and z become the Nambu-Goldstone bosons which are to be absorbed into the longitudinal part of the gauge bosons $W^\pm$ and Z respectively. The other mass-eigenstates h^0, H^0, $H^\pm$, and A^0 become to represent five massive Higgs bosons, that is, two CP-even neutral, charged and CP-odd neutral ones, respectively. Another mixing angle α is chosen in order that h^0 is lighter than H^0. The relation between the coupling constants and masses are

$$\eta_1 = \frac{1}{2v^2\cos^2\beta}(\cos^2\alpha\, m_{H^0}^2 + \sin^2\alpha\, m_{h^0}^2 - \tan\beta\, \mu_3^2), \tag{3}$$

$$\eta_2 = \frac{1}{2v^2\sin^2\beta}(\sin^2\alpha\, m_{H^0}^2 + \cos^2\alpha\, m_{h^0}^2 - \cot\beta\, \mu_3^2), \tag{4}$$

$$\eta_3 = \frac{\sin 2\alpha}{v^2\sin 2\beta}(m_{H^0}^2 - m_{h^0}^2) + \frac{2m_{H^\pm}^2}{v^2} - \frac{2}{v^2\sin 2\beta}\,\mu_3^2, \tag{5}$$

$$\eta_4 = -\frac{2m_{H^\pm}^2}{v^2} + \frac{4}{v^2\sin 2\beta}\,\mu_3^2, \tag{6}$$

$$\eta_5 = \frac{2}{v^2}(m_{A^0}^2 - m_{H^\pm}^2). \tag{7}$$

Note that since only the η_5-term explicitly breaks the custodial $SU(2)_V$ symmetry in the Higgs sector, Eq (7) implies that the mass splitting between $H^\pm$ and A^0 measures the $SU(2)_V$ breaking. The eight independent parameters $(\mu_1, \mu_2, \mu_3, \eta_1, \sim, \eta_5)$ in (1) are thus

[3] As we mention later, the severe constraint of the ρ-parameter from the present data do not always forbid the large breaking of the custodial symmetry in the THDM Higgs sector completely.

replaced into the four mass parameters $m_{h^0}, m_{H^0}, m_{H^\pm}$ and m_{A^0}, the two mixing angles α and β, the vacuum expectation value v and the soft-breaking parameter μ_3.

Next, we discuss the non-decoupling effects of the Higgs bosons in this model. In case of the fermion sector, the Yukawa coupling constants are naively proportional to fermion masses. This implies that the masses of fermions are enhanced only by the growing Yukawa coupling constants. Then the decoupling theorem does not work and the non-decoupling effects of fermion masses appear. In case of the SM Higgs sector, the similar effects are expected because the quartic self-coupling constant is proportional to the Higgs boson mass [17]. On the other hand, in case of the THDM Higgs sector, whether the heavy Higgs bosons but the lightest in the loop are decoupled or not is a model dependent problem. For example, the mass of A^0 is given from Eqs. (6) and (7) as

$$m_{A^0}^2 = \frac{1}{2}(\eta_5 - \eta_4)v^2 + \frac{1}{\sin\beta\cos\beta}\,\mu_3^2. \tag{8}$$

Naively, m_{A^0} can become large by the growing quartic coupling constants or the large soft-breaking parameter μ_3^2. If large m_{A^0} is realized by the μ_3^2 term with keeping the quartic coupling constants to be small, the Higgs boson masses then become to be decoupled. Note that the MSSM Higgs sector belongs to this type, in which all the quartic coupling constants are constrained to $\mathcal{O}(g^2)$, where g is the weak gauge coupling constants, so that all the heavy Higgs bosons (H^0, $H^\pm$ and A^0) can grow only due to the large soft-breaking parameters. Alternatively, if large m_A is realized by the large quartic coupling constants with keeping μ_3^2 to be small, the similar situation to the fermion and SM Higgs case occurs. Thus non-decoupling contributions of Higgs boson masses are expected in these cases [18]. We note that the non-decoupling Higgs theories often receive strong constraints on the Higgs boson masses by the perturbative unitarity [24].

The situation that Higgs boson masses mainly come from the self-coupling constant is, by itself, also seen in the case of SM. The non-decoupling effects of the Higgs boson are then induced in, for example, the oblique corrections. However, in the SM case, the Higgs sector with the one Higss doublet is custodial $SU(2)_V$ symmetric. The leading power-like contributions of the Higgs bosons are canceled due to this symmetry and at most the sub-leading logarithmic contribution ($\sim \log m_H$) appears. This phenomenon in the oblique

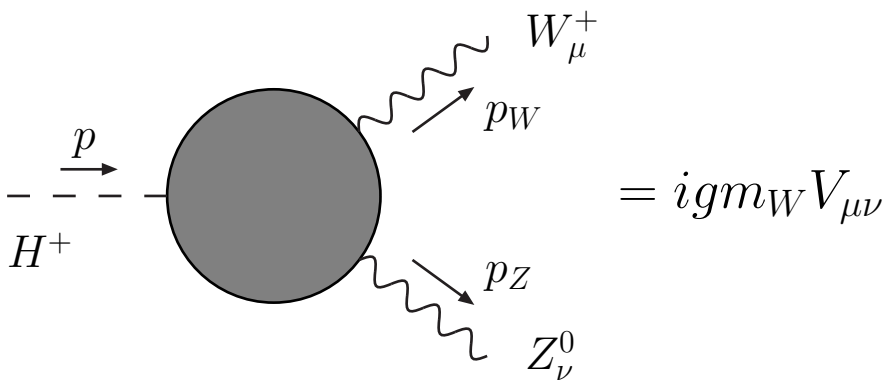

Fig 1.

corrections has been known as the screening theorem [20]. In THDM, there can be leading power-like contributions of Higgs boson masses in the case without the custodial symmetry. In this paper, we study the possibility that the enhancement of the loop induced $H^\pm W^\mp Z^0$ vertex may occur by the similar mechanism.

3 Non-decoupling Effects on Loop Induced $H^\pm W^\mp Z^0$ vertex

The $H^\pm W^\mp Z^0$ vertex is defined as $igm_W V_{\mu\nu}$ (See Fig 1.), where $V_{\mu\nu}$ is expressed by [10]

$$V_{\mu\nu} = F g_{\mu\nu} + \frac{G}{m_W^2} p_{Z\mu} p_{W\nu} + \frac{H}{m_W^2} \epsilon_{\mu\nu\rho\sigma} p_Z^\rho p_W^\sigma, \tag{9}$$

where p_Z and p_W are momenta of Z and W bosons, respectively. All the external lines are assumed to be on mass-shell. We have $\partial_\mu W^\mu = 0$ and $\partial_\mu Z^\mu = 0$ then.

First of all, we observe the absence of the $H^\pm W^\mp Z^0$ coupling at tree level in THDM. The tree-level coupling is considered to be generated in the kinetic part of the Higgs sector,

$$\mathcal{L}^{kin}_{\rm THDM} = \sum_{i=1}^{2} (D_\mu \Phi_i)^\dagger D^\mu \Phi_i, \tag{10}$$

where D_μ is the covariant derivative for $SU(2)_L \otimes U(1)_Y$. In the Georgi basis [29], which is obtained from Φ_i rotating by β, Eq (10) becomes

$$\mathcal{L}^{kin}_{\rm THDM} = (D_\mu \Phi)^\dagger D^\mu \Phi + (D_\mu \Psi)^\dagger D^\mu \Psi, \tag{11}$$

where

$$\Phi = \begin{pmatrix} w^+ \\ \frac{1}{\sqrt{2}}(\phi^0 + v + iz^0) \end{pmatrix}, \Psi = \begin{pmatrix} H^+ \\ \frac{1}{\sqrt{2}}(\psi^0 + iA^0) \end{pmatrix}, \tag{12}$$

and

$$\phi^0 = \cos(\alpha-\beta)H^0 - \sin(\alpha-\beta)h^0, \tag{13}$$

$$\psi^0 = \sin(\alpha-\beta)H^0 + \cos(\alpha-\beta)h^0. \tag{14}$$

Since Ψ does not have any vacuum expectation value and there is no mixing between Φ and Ψ in Eq (11), we can understand the absence of $H^\pm W^\mp Z^0$ at the tree level. The $H^\pm W^\mp Z^0$ vertex can induced only by the loop level where the mixing between Φ and Ψ is induced through effects from the other sectors.

Second, we discuss the non-decoupling effects of heavy particles on the vertex. The effective Lagrangian is

$$\begin{aligned} \mathcal{L}_{\rm eff} &= f_{H^+W^-Z^0} H^+ W^-_\mu Z^\mu + \text{h.c.} \\ &+ g_{H^+W^-Z^0} H^+ F_Z^{\mu\nu} F^W_{\mu\nu} + \text{h.c.} \\ &+ h_{H^+W^-Z^0}\ i\epsilon_{\mu\nu\rho\sigma} H^+ F_Z^{\mu\nu} F_W^{\rho\sigma} + \text{h.c.}. \end{aligned} \tag{15}$$

Since the coefficient $f_{H^+W^-Z^0}$ is mass-dimension one, the contribution of the heavy particles with the masses M_i take the form at one loop level like

$$f_{H^+W^-Z^0} \sim g \times \frac{g}{\cos\theta_W} \times \frac{M_i^2}{v} \times f(M_i) \sim \frac{m_W m_Z}{v^3} \times M_i^2 f(M_i), \tag{16}$$

where $f(M_i)$ is a dimensionless function of M_i's. Hence the leading contributions of heavy masses to $f_{H^+W^-Z^0}$ are expected to be quadratic ones. As for the dimension -1 coefficients $g_{H^+W^-Z^0}$ and $h_{H^+W^-Z^0}$, they are expected to take the forms at one loop level like

$$g_{H^+W^-Z^0},\ h_{H^+W^-Z^0} \sim \frac{m_W m_Z}{v^3} \times f'(M_i), \tag{17}$$

where $f'(M_i)$ is a dimensionless function of M_i's. Namely they have the Higgs mass contributions like at most $\sim \log M_i$. Therefore from the naive power counting, we expect that there may be non-decoupling effects (quadratic and logarithmic mass contributions)

of the heavy Higgs bosons as well as heavy fermions at the one loop induced $H^{\pm}W^{\mp}Z^0$ vertex [4].

Third, we show that the the non-decoupling effects on the vertex is strongly constrained if there is the custodial $SU(2)_V$ symmetry. In our model, the effective Lagrangian (15) comes from the operators,

$$\mathrm{tr}\left[\tau_3(D_\mu\mathcal{M})^\dagger(D^\mu\mathcal{N})\right],\ \ \mathrm{tr}\left[\tau_3\mathcal{M}^\dagger\mathcal{N}F_Z^{\mu\nu}F_{\mu\nu}^W\right]\ \text{and}\ \ i\epsilon_{\mu\nu\rho\sigma}\mathrm{tr}\left[\tau_3\mathcal{M}^\dagger\mathcal{N}F_Z^{\mu\nu}F_W^{\rho\sigma}\right], \tag{18}$$

where 2×2 matrices $\mathcal{M}$ and $\mathcal{N}$ are defined by using the doublets Φ and Ψ in (12) as $\mathcal{M}=(i\tau_2\Phi^*,\Phi)$ and $\mathcal{N}=(i\tau_2\Psi^*,\Psi)$. Since it can be seen clearly that all the operators (18) are un-invariant under $SU(2)_R$ and thus $SU(2)_V$, we understand that the vertex appears only in the case without the custodial $SU(2)_V$ symmetry.

In our model, there are three independent sources for the explicit $SU(2)_V$ breaking according to the gauge, fermion and Higgs sectors. They are separately measured by the three mass-splittings $m_W^2-m_Z^2$, $m_t^2-m_b^2$ and $m_A^2-m_{H^\pm}^2$, respectively. Since the breakdown in the gauge as well as the fermion sectors is already known experimentally, the quadratic mass contributions of the gauge bosons and fermions appear in the vertex. In MSSM, only the effects of the heavy fermions (especially the top-quark) become important because the explicit breaking of $SU(2)_V$ in both the gauge and Higgs sectors are small. However, in the present situation that the top-quarks has been already discovered with the mass of ~ 175 GeV [12] and the forth generation of quarks has almost been excluded by the S-parameter constraints [2, 13], it seems to be difficult to obtain a substantial enhancement of the vertex only by the fermion effects. Hence the only hope to the novel enhancement of the vertex is due to the non-decoupling Higgs sector with enough large mass splitting $m_{A^0}-m_{H^\pm}$.

Finally we note that, as well known, the experimental value of ρ parameter gives a strong constraint for the breaking of the custodial symmetry. Even in THDM, the large parameter region have been already excluded by the data [2, 23]. We, however, stress

[4]Since there is no correspondence to $f_{H^+W^-Z^0}$ term in the effective Lagrangian for the $H^{\pm}W^{\mp}\gamma$ vertex because of the gauge invariant condition $p_\gamma^\mu V_{\mu\nu}=0$, the quadratic mass effects disappear in the one loop induced $H^{\pm}W^{\mp}\gamma$ vertex [11]. Thus the large enhancement of the vertex cannot be expected in this vertex and this fact is the reason what we consider only the $H^{\pm}W^{\mp}Z^0$ vertex.

that the ρ parameter constraint does not always forbid large $SU(2)_V$ breaking in the THDM Higgs sector. For one of the examples, if we consider the case with $\alpha - \beta \sim \pi/2$ and $m^2_{H^\pm} \sim m^2_{H^0}$, the large mass splitting between A^0 and $H^\pm$ is possible with keeping $\Delta\rho = \rho - 1 \sim 0$.

Thus it becomes important and very interesting to study the non-decoupling effects of the Higgs bosons on the vertex. It is possible that $m^2_A - m^2_{H^\pm}$ is large enough to give substantial non-decoupling effects such as $\sim M_i^2$ on the vertex with keeping $\Delta\rho \sim 0$.

4 Analysis of $H^+ \to W^+ Z^0$

In Sec 3, we have qualitatively discussed the possibility that the loop-induced $H^\pm W^\mp Z^0$ vertex can be significantly enhanced by the Higgs non-decoupling effects if there is large explicit breaking of the custodial $SU(2)_V$ symmetry in the Higgs sector. To verify this observation quantitatively, we proceed to the analysis of the decay process $H^+ \to W^+ Z^0$. We here present the one-loop calculation of the decay width and evaluate the branching ratio of this decay mode. The decay width is given in terms of the form factors F, G and H (see Eq (9)) as [10]

$$\Gamma(H^+ \to W^+ Z^0) = m_{H^\pm} \frac{\lambda^{1/2}(1,w,z)}{16\pi} \left(|\mathcal{M}_{LL}|^2 + |\mathcal{M}_{TT}|^2 \right), \tag{19}$$

where $w = (m_W/m_{H^\pm})^2$, $z = (m_Z/m_{H^\pm})^2$, $\lambda(a,b,c) = (a-b-c)^2 - 4bc$. The amplitudes $\mathcal{M}_{LL}$ and $\mathcal{M}_{TT}$ are the contributions of each modes of the longitudinally and transversely polarized final gauge bosons. We have their explicit expressions,

$$|\mathcal{M}_{LL}|^2 = \frac{g^2}{4z} \left| (1-w-z)F + \frac{\lambda(1,w,z)}{2w} G \right|^2 \tag{20}$$

$$|\mathcal{M}_{TT}|^2 = g^2 \left\{ 2w|F|^2 + \frac{\lambda(1,w,z)}{2w} |H|^2 \right\}. \tag{21}$$

The contributions of the diagrams with a boson (Higgs, Nambu-Goldstone or gauge bosons) loop are calculated by employing the t'Hooft-Feynman gauge here. The boson-loop diagrams are shown in Figs 2(a), (b) and (c). The explicit expressions of these boson-loop contributions to the quantities F and G are given in Appendix 1. All the boson-loop diagrams do not contribute to the quantity H at all because the boson sectors of the theory

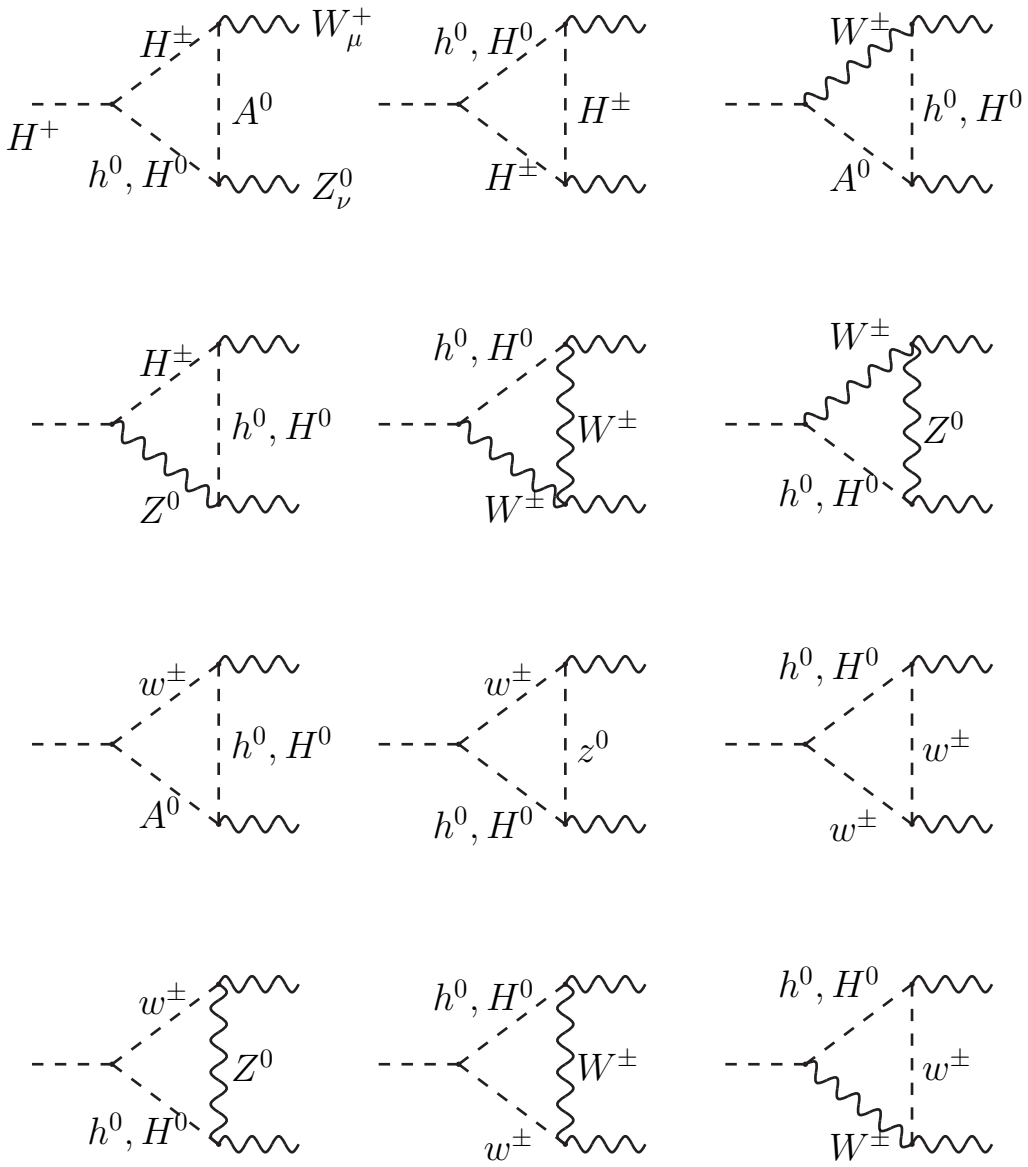

Fig 2-a

has the parity (P) symmetry. The fermion-loop diagrams are shown in Fig 2(d). Since all the diagrams with a fermion-loop themselves construct a gauge invariant subset, we are free to use different gauge choices for boson- and fermion-loops. It is clear that the unitary gauge is the most convenient choice for the contributions of the fermion-loop diagrams. The explicit calculations of the fermion-loop contribution are given in Ref [11]. We have

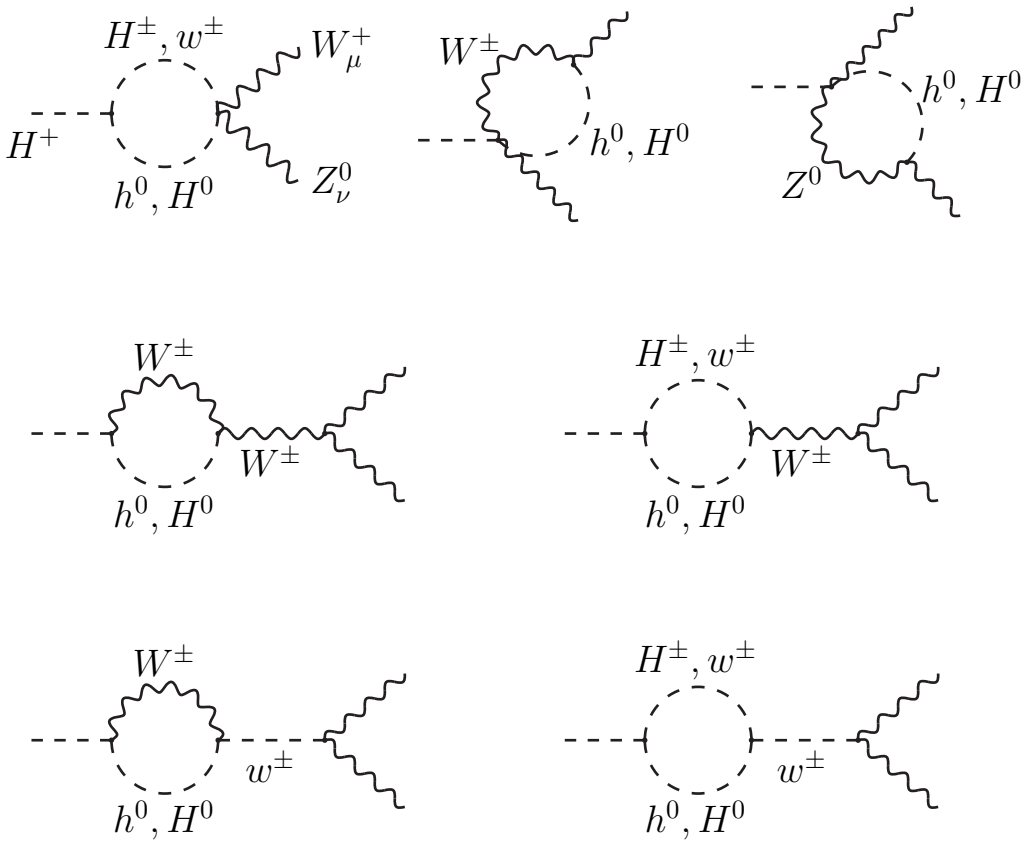

Fig 2-b

just checked their results.

4.1 Heavy mass limit

We consider to extract the contribution of the masses of heavy Higgs bosons. In this subsection, we assume that both the neutral (h^0, H^0) and CP-odd (A^0) Higgs bosons are heavier than the charged one. The soft-breaking parameter μ_3^2 is also set into zero for a while in order to obtain the non-decoupling effects of the Higgs bosons maximally.

A naive counting by using Eqs (20) and (21) shows that the ratio $|\mathcal{M}_{TT}/\mathcal{M}_{LL}|^2$ behaves like $\sim 8 \cdot m_W^2/m_{H^\pm}^2 \cdot m_Z^2/m_{H^\pm}^2$. If $m_{H^\pm}^2/m_W^2$ is large, the contribution of $\mathcal{M}_{LL}$ becomes dominant. The bosonic loop contributions to $\mathcal{M}_{LL}$ can rewritten by factorizing the mixing

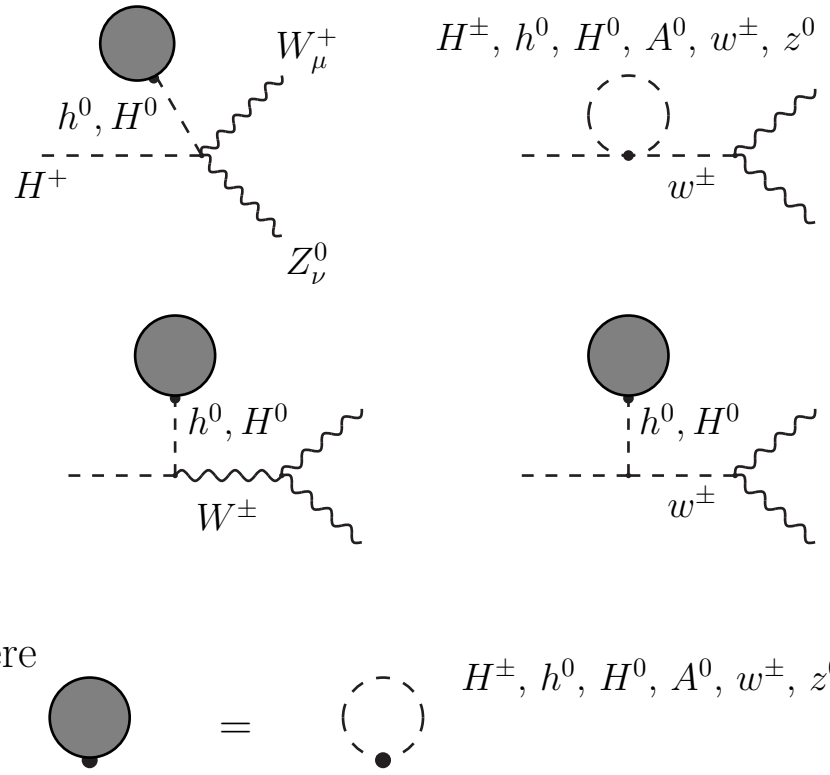

Fig 2-c

angle dependence as

$$\mathcal{M}_{LL} = J(\alpha,\beta)\mathcal{M}^J_{LL}(M_i) + K(\alpha,\beta)\mathcal{M}^K_{LL}(M_i) + L(\alpha,\beta)\mathcal{M}^L_{LL}(M_i), \tag{22}$$

where M_i represent the masses of h^0, H^0 and A^0, and

$$J(\alpha,\beta) = \sin(\alpha-\beta)\cos(\alpha-\beta), \tag{23}$$

$$K(\alpha,\beta) = \sin^2\alpha\cot\beta - \cos^2\alpha\tan\beta, \tag{24}$$

$$L(\alpha,\beta) = \cos^2\alpha\cot\beta - \sin^2\alpha\tan\beta. \tag{25}$$

The leading (quadratic) mass effects of heavier Higgs bosons on $\mathcal{M}^J_{LL}(M_i)$, $\mathcal{M}^K_{LL}(M_i)$ and $\mathcal{M}^L_{LL}(M_i)$ are then extracted from the full expression in Appendix 1 as

$$\mathcal{M}^J_{LL}(M_i) \sim 0, \tag{26}$$

$$\mathcal{M}^K_{LL}(M_i) \sim \frac{m_{H^\pm}}{2(4\pi)^2 v^3} \times \frac{m^2_{H^0} m^2_{A^0}}{m^2_{H^0} - m^2_{A^0}} \ln\frac{m^2_{H^0}}{m^2_{A^0}}, \tag{27}$$

$$\mathcal{M}^K_{LL}(M_i) \sim \frac{m_{H^\pm}}{2(4\pi)^2 v^3} \times \frac{m^2_{h^0} m^2_{A^0}}{m^2_{h^0} - m^2_{A^0}} \ln\frac{m^2_{h^0}}{m^2_{A^0}}. \tag{28}$$

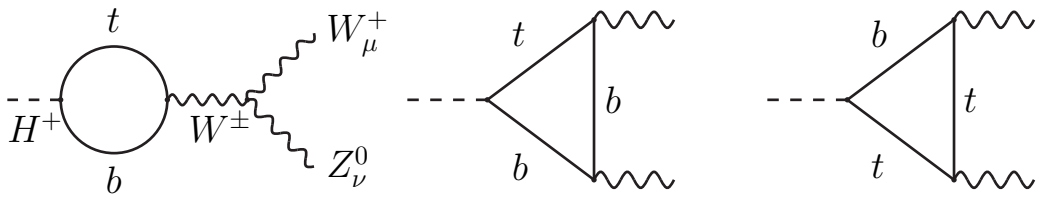

Fig 2-d

Eq (22) shows that the vertex can be strongly enhanced by the Higgs mass effects if $\tan\beta$ or $\cot\beta$ is large enough. [5]

The results in Eqs (26) $\sim$ (28) are also reproduced from the much simpler calculation of $H^+ \to w^+ z^0$ by virtue of the equivalence theorem [30, 31]. The calculation in this way is performed by the Landau gauge [19] and the diagrams are shown in Fig 3. We show the explicit form of the amplitude calculated in this way in Appendix 2. To take the heavy mass limit in this amplitude leads to the completely same results as Eqs (26) $\sim$ (28). The use of the equivalence theorem is very useful to check the results of the full calculation (See Fig 7(a) and (b).). One more advantage of the use of the equivalence theorem here is the fact that we can immediately see the disappearance of the amplitudes if the Higgs sector is custodial $SU(2)_V$ symmetric. All the diagrams in Fig 3 have a coupling of $H^\pm w^\mp A^0$ (shown by the brack dot in each diagram). The coupling constant is just η_5 ($\propto m^2_{A^0} - m^2_{H^\pm}$) which represents the explicit breaking of $SU(2)_V$ in the Higgs sector.

4.2 Numerical Estimation

The decay width $\Gamma(H^+ \to W^+ Z^0)$ is evaluated by using Eqs (19), (20) and (21). For comparison, the MSSM (with heavy sparticles) case and the non-decoupling THDM case are shown in Fig 4(a) and 4(b), respectively. In MSSM, the heavy Higgs bosons are approximately degenerated ($m_{H^\pm} - m_{A^0} < 11$ GeV for $m_{H^\pm} > 300$ GeV). Hence the Higgs

[5] In MSSM, the soft-breaking term μ_3^2 cannot be neglected and the mixing angles are not independent of each other. In the large mass limit, we have $m^2_{A^0} \sim m^2_{H^\pm} \sim m^2_{H^0} \sim 2\mu_3^2/\sin 2\beta$ and $\alpha = \beta - \pi/2$. The enhancement mentioned above can no longer appear in this case because of the cancellation due to the soft breaking parameter. In general THDM, this cancellation do not have to take place as in the cases above.

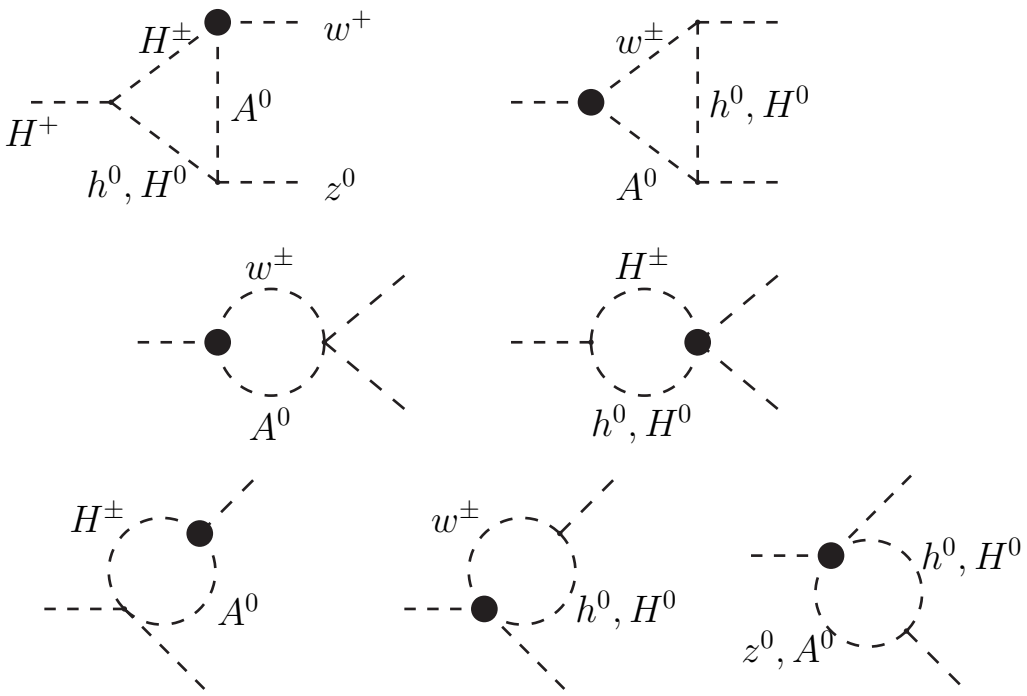

Fig 3

effects are small and heavy fermion (top-quark) effects are dominant. Since the $H^{\pm}tb$ coupling consists of $\sim m_t \cot\beta$ and $m_b \tan\beta$, the top-quark contributions are rapidly reduced for larger $\tan\beta$. We can see from Fig 4(a) that $\Gamma(H^+ \to W^+Z^0) < 10^{-3}$ at $m_{H^{\pm}} = 300$ GeV for $\tan\beta > 1$. These results for MSSM are quitely consistent with the previous ones [10, 11]. On the other hand, in Fig 2(b), in case of THDM with $m_{H^{\pm}} - m_{A^0} =$ 200 GeV, the novel enhancement of the width is realized for large $\tan\beta$ due to the Higgs non-decoupling effects (we are setting μ_3 into zero here). In Fig 5, we show the $\tan\beta$ dependence of $\Gamma(H^+ \to W^+Z^0)$ for various mass splitting $\Delta m = |m_{A^0} - m_{H^{\pm}}|$. The enhancement in small $\tan\beta$ region ($\tan\beta < 1$) is due to the top quark contribution, while the width can be considerably enhanced even for large $\tan\beta$ regions by the Higgs non-decoupling effects if Δm become large enough.

We next consider the branching ratio. The decay mode is kinematically allowed if $m_{H^{\pm}} > m_W + m_Z$. This is very close to the threshold of tb mode with the top-quark mass

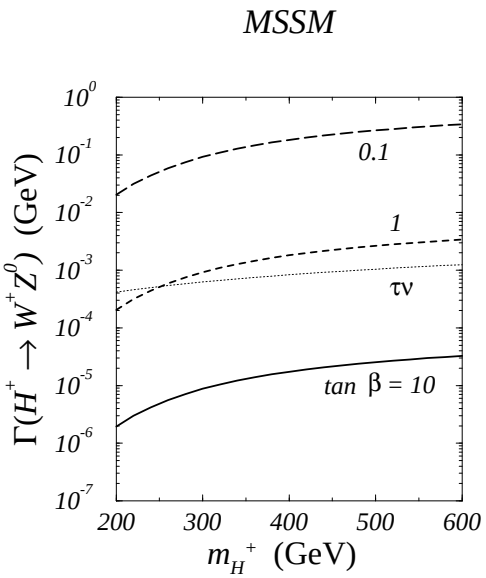

Fig 4(a): Decay width $\Gamma(H^+ \to W^+Z^0)$ for $\tan\beta = 0.1, 1, 10$ in MSSM (All the sparticles are assumed to be very heavy). The decay width of $H^+ \to \bar{\tau}\nu$ for $\tan\beta = 1$ is also shown for comparison.

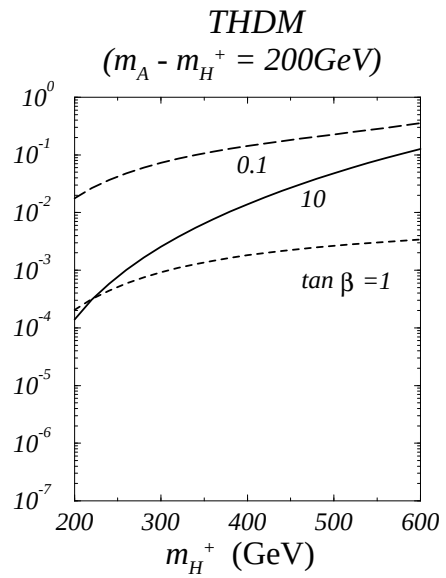

Fig 4(b): $\Gamma(H^+ \to W^+Z^0)$ for $\tan\beta = 0.1$, 1 and 10 in THDM with $m_{A^0} - m_{H^\pm} = 200$ GeV. The other parameters are taken as $\alpha = \beta - \pi/2$, $m_{H^0} = m_{H^\pm} + 10$ GeV, $m_{h^0} = 140$ GeV and $\mu_3 = 0$.

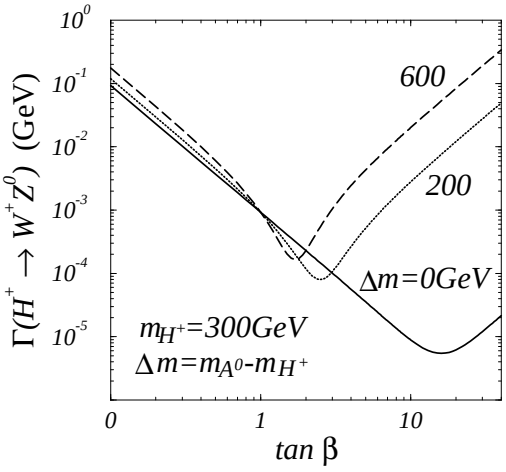

Fig 5: $\Gamma(H^+ \to W^+Z^0)$ at $m_{H^\pm} = 300$ GeV as a function of $\tan\beta$. $\Delta m = m_{A^0} - m_{H^\pm}$ is set into 0, 200 or 600 GeV. The other parameters are taken as $\alpha = \beta - \pi/2$, $m_{H^0} = 310$ GeV, $m_{h^0} = 140$ GeV and $\mu_3 = 0$.

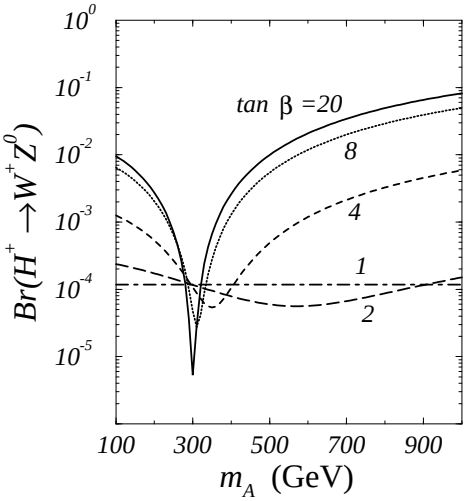

Fig 6(a): $Br(H^+ \to W^+Z^0)$ in THDM for $m_{H^\pm} = 300$ GeV as a function of m_{A^0}. Other parameters are chosen as $\alpha = \beta - \pi/2$, $m_{H^\pm} = 310$ GeV, $m_{h^0} = 140$ GeV and $\mu_3 = 0$.

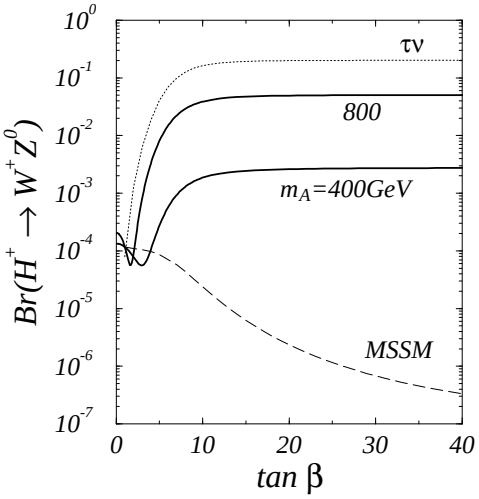

Fig 6(b): $Br(H^+ \to W^+Z^0)$ in THDM for $m_{H^\pm} = 300$ GeV as a function of $\tan\beta$ (Solid lines). Other parameters are chosen as the same as Fig 6(a).

~ 175 GeV [2, 12]. In addition, there is a lower bound for the charged Higgs boson in Type II THDM from the $b \to s\gamma$ measurement as $m_{H^\pm} > 244 + 63/(\tan\beta)^{1.3}$ [7]. We assume here that the charged Higgs boson is heavy enough to open the tb mode, which becomes the most dominant mode then. The other modes to be considered are $H^\pm \to \tau\nu$, cs and $h^0W^\pm$ (if it is allowed). Their decay widths at tree level behave like

$$\Gamma(H^\pm \to tb) \sim N_C(m_t^2 \cot^2\beta + m_b^2 \tan^2\beta), \tag{29}$$

$$\Gamma(H^\pm \to cs) \sim N_C(m_c^2 \cot^2\beta + m_s^2 \tan^2\beta), \tag{30}$$

$$\Gamma(H^\pm \to \tau\nu) \sim m_\tau^2 \tan^2\beta, \tag{31}$$

$$\Gamma(H^\pm \to h^0W^\pm) \sim m_W^2 \cos^2(\alpha - \beta), \tag{32}$$

The region of variables are taken as $200 < m_{H^\pm} < 800$ GeV, $100 < m_{A^0} < 900$ GeV and $1 < \tan\beta < 50$. The other parameters are fixed as $m_{h^0} = 140$ GeV, $m_{H^0} = 310$ GeV and $\alpha = \beta - \pi/2$. As to the fermion masses, we assume that $m_t = 175$ GeV and $m_b(m_{H^\pm}) = 3$ GeV [32]. The reason for this parameter choice is the ρ-parameter constraint. From the data from LEP experiments, we can evaluate the contribution of the Higgs sector; $\Delta\rho_{THDM}$

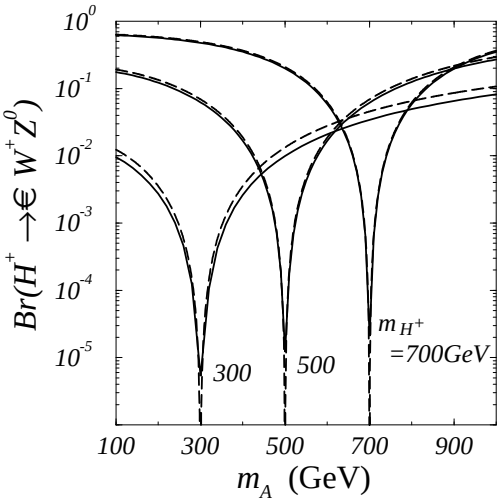

Fig 7(a): $Br(H^+ \to W^+Z^0)$ for various values of $m_{H^\pm}$ as a function of m_{A^0}. The other parameters are chosen as $\tan\beta = 20$, $\alpha = \beta - \pi/2$, $m_{H^0} = m_{H^\pm} + 10$ GeV, $m_{h^0} = 140$ GeV and $\mu_3 = 0$. Solid lines are the results of the full calculation. Dashed lines are those of the calculation by using the equivalence theorem.

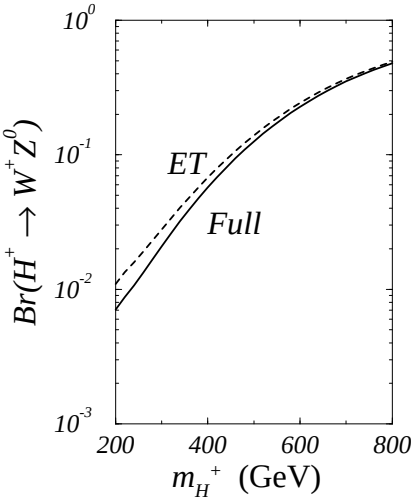

Fig 7(b): $Br(H^+ \to W^+Z^0)$ for $\tan\beta = 20$. Other parameters are chosen as $\tan\beta = 20$, $\alpha = \beta - \pi/2$, $m_{A^0} = m_{H^\pm} + 300$ GeV, $m_{H^0} = m_{H^\pm} + 10$ GeV, $m_{h^0} = 140$ GeV and $\mu_3 = 0$. The results from the full calculation (Full) and the results by using the equivalence theorem (ET) are shown.

$\sim -0.00180 \pm 0.00204$ (2σ) [2]. The other constraints for $\tan\beta$ from $B^0 - \bar{B}^0$ mixing [33] and for $m_{H^\pm}$ from $b \to s\gamma$ [7] are also in our consideration here. Moreover, we take account of the constraint from the perturbative unitarity for the Higgs boson masses [24].

In Fig 6, we show the branching ratio $Br(H^\pm \to W^\pm Z^0)$ at $m_{H^\pm} = 300$ GeV. We can see in Fig 6(a) that the branching ratio become larger than 10^{-2} if the mass splitting between $H^\pm$ and A^0 is greater than 200 GeV for $\tan\beta > 5 \sim 8$. The maximal value of $Br(H^\pm \to W^\pm Z^0)$ can amount to near 10^{-1} for very large m_{A^0} and $\tan\beta > 20$. In the nearly $SU(2)_V$ symmetric cases in the Higgs sector ($m_{A^0} \sim m_{H^\pm}$), the Higgs non-decoupling effects are canceled out and only the fermion and gauge boson contributions remain, so that the branching ratio becomes smaller than 10^{-4}. Since the top-quark mass contributions are decreased and the Higgs mass contributions are increased as $\tan\beta$ grows,

the cancellation of the Higgs contributions become more clear for large $\tan\beta$. On the other hand, at near $\tan\beta \sim 1$, the top-quark mass contribution becomes much dominant and thus we can see nothing happens at $m_{H^\pm} = m_{A^0}$. The $\tan\beta$ dependence is shown in Fig 6(b) for $m_{H^\pm} = 300$ GeV. The other parameters are taken as same as Fig 6(a). We also show there $Br(H^+ \to W^+Z^0)$ in the MSSM case for a comparison, in which the Higgs mass effects is almost suppressed by the approximate $SU(2)_V$ in the Higgs sector. For further comparison, the results of $Br(H^+ \to \tau\nu)$ are also attached in Fig 6(b). The branching ratios for various values of $m_{H^\pm}$ are shown in Fig 7(a) and (b). The similar properties to $m_{H^\pm} \sim 300$ GeV are seen for each value of $m_{H^\pm}$ in Fig 7(a). Both the results by the full calculation and the calculation simplified by virtue of the equivalence theorem are presented there. We can see that the latter results become an excellent approximation to the full calculation for larger values of $m_{H^\pm}$ especially in Fig 7(b).

We have shown that, in general THDM, the loop induced $H^\pm W^\mp Z^0$ vertex can be considerably enhanced due to the non-decoupling effects of the Higgs bosons. All the analyses above have been considered by making the soft-breaking parameter μ_3^2 to be zero because we have tried to extract the Higgs non-decoupling effects as large as possible. However, the soft-breaking parameter μ_3^2 often become very important in various aspects of physics. First of all, it cannot be neglected in MSSM case. Second, if we are interested in the Higgs sector as an additional CP violating source, μ_3^2 is the parameter which can be considered to have a phase [27]. Finally, since $\mu_3^2 = 0$ implies that there is the exact discrete symmetry in the Higgs sector which is spontaneously broken according to the gauge symmetry breaking. In that case, the problem of the domain wall takes place [34]. To avoid this, the discrete symmetry may have to be explicitly broken (but only softly for FCNC suppression) by the non-zero μ_3^2 parameter. As we mentioned in Sec 3, the heavier Higgs boson masses have two kinds of origin, namely, the quartic coupling constant times the vacuum expectation value and the soft-breaking term. The non-zero soft-breaking term reduces the contribution of the quartic couplings for a fixed masses, so that the non-decoupling effects are suppressed to some extent. We show the relation between the non-decoupling effects and the non-zero soft-breaking parameter on the branching ratio in Fig 8. The Higgs

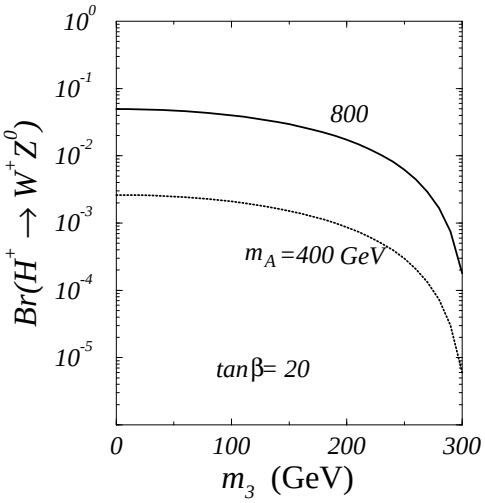

Fig 8: The soft-breaking parameter dependence of $Br(H^+ \to W^+Z^0)$ at $m_{H^\pm} = 300$ GeV. The parameter m_3 is defined by $m_3^2 \equiv \mu_3^2/\cos\beta\sin\beta$. Other parameters are chosen as $\alpha = \beta - \pi/2$, $m_{H^0} = 310$ GeV and $m_{h^0} = 140$ GeV.

non-decoupling limit ($m_3^2 \equiv \mu_3^2/\sin\beta\cos\beta \sim 0$) is what we have seen in the previous figures. In the case of $m_3 \sim 300$ GeV ($= m_{H^\pm}$), in which the heavier Higgs bosons receive their masses only from μ_3^2, the complete cancellation of the non-decoupling effects of Higgs boson masses takes place and the model becomes the decoupling theory for the heavy Higgs bosons just like in MSSM.

5 Discussion and Conclusion

We have discussed the loop-induced $H^\pm W^\mp Z^0$ vertex in Type II THDM and its enhancement due to the non-decoupling effects of the heavy Higgs as well as the heavy quarks. The conditions for the large enhancement due to the Higgs mass effects have been summarized as 1) the large Higgs masses coming from the larger contributions of the quartic coupling constants with keeping the soft-breaking parameter to be smaller, 2) the large explicit breaking of $SU(2)_V$ in the Higgs sector by the large mass splitting between $H^\pm$ and A^0. In the case of MSSM, since both the conditions above are impossible,

such the Higgs mass effects do not take place and any substantial enhancement cannot be realized. The decay width $\Gamma(H^+ \to W^+ Z^0)$ remains $< 10^{-3}$ GeV at $m_{m^\pm} = 300$ GeV for $\tan\beta > 1$. On the other hand, in the case of THDM, the conditions can be satisfied within the constraint from the available experimental data. We have found that the decay width $\Gamma(H^\pm \to W^+ Z^0)$ can amount to $> 10^{-1}$ GeV at $m_{H^\pm} \sim 300$ GeV for large $\tan\beta$. These values are considered to be much larger ($\sim 10^1 - 10^2$) than the typical values in the E_6 model, in which a tree $H^\pm W^\mp Z^0$ coupling can be induced through $Z - Z'$ mixing [35] and also smaller ($\sim 10^{-2} - 10^{-1}$) than those in the model with a doublet and two (a real and a complex) triplets [14]. In Type II THDM, since $m_{H^\pm}$ is constrained to be larger than ~ 250 GeV for large $\tan\beta$ by $b \to s\gamma$ data, $H^\pm \to tb$ opens and becomes the most dominant mode. We have evaluated the branching ratio and found that, even in such the situation, it can amount to $10^{-2} \sim 10^{-1}$ at $m_{H^\pm} = 300$ GeV within the constraints from the present experimental data and also the perturbative unitarity.

Such the enhancement may make it possible to detect the decay mode at LHC or (if fortune) LC's. The charged Higgs boson is mainly produced through the subprocess $gb \to tH^\pm$ [36] at LHC. We expect that, if $m_{H^\pm}$ is 300 GeV, about 200 (50) events of $H^\pm \to W^\pm Z^0 \to lll\nu$ are produced for $\tan\beta = 1$ (20) per a year at LHC with the integrated luminosity $\sim 2 \times 10^2$ fb^{-1}/year. Since the background (mainly $ud \to W^\pm Z^0$) has been naively estimated to be such that a few % of the branching ratios are required to see a signal, we can expect to detect the decay mode if such the large enhancement occurs. At the future e^+e^- linear collider with $\sqrt{s} = 1$ TeV and the integrated luminosity ~ 50 fb^{-1}/year, a few thousands of $H^\pm$ are expected to be produced through $e^+e^- \to H^+H^-$. The decay $H^\pm \to W^\pm Z^0$ with the maximally enhanced branching ratio (near 10 %) might be also detectable there because less background would be expected.

Acknowledgments

The author would like to thank Yasuhiro Okada and Kaoru Hagiwara for valuable discussions and useful comments, Chung Kao, Hide-Aki Tohyama, Minoru Tanaka and Seiji Matsumoto for helpful discussions. This work was supported, in part, by Grant-in-Aid for Scientific Research from the Ministry of Education, Science and Culture of Japan.

APPENDICES

APPENDIX 1: Calculation of Boson-Loop Contribution

Here we show the explicit results of the calculation of the loop induced $H^{\pm}W^{\mp}Z^0$ vertex. As shown in Eq (9), the contributions are expressed in terms of the quantities F, G and H. They can be divided as

$$X = X^{(\mathrm{a})} + X^{(\mathrm{b})} + X^{(\mathrm{c})} + X^{(\mathrm{d})}, \tag{A.1}$$

where X represents F, G or H. $X^{(\mathrm{a}\sim\mathrm{d})}$ correspond to the diagrams in Fig 2(a) $\sim$ (d), respectively. We employ the 't Hooft-Feynman gauge for calculation of the boson-loop diagrams. Explicit forms for $X^{(\mathrm{a})\sim(\mathrm{c})}$ are listed in the following. The contribution of fermion-loop diagrams $X^{(\mathrm{d})}$ have been calculated in the unitary gauge and their explicit expressions are given in Ref [11]. As mentioned before, the diagrams with a fermion loop, by themselves, form the gauge invariant sub-set, so that we can use these results consistently. The contributions of the boson-loop diagrams are expressed in terms of the integral functions [37], whose definition here is beased on the second paper of Ref [2].

$$\begin{aligned}
F^{(\mathrm{a})} &= \frac{2}{16\pi^2 v^2 \cos\theta_W} \\
&\times \Bigg[-\left\{ K(\alpha,\beta) m_{H^0}^2 + J(\alpha,\beta)(-m_{H^0}^2 + 2m_{H^\pm}^2) - \frac{\sin(\alpha+\beta)}{\sin\beta\cos\beta} m_3^2 \right\} C_{24}[H^\pm A^0 H^0] \\
&- \left\{ L(\alpha,\beta) m_{h^0}^2 - J(\alpha,\beta)(-m_{h^0}^2 + 2m_{H^\pm}^2) - \frac{\cos(\alpha+\beta)}{\sin\beta\cos\beta} m_3^2 \right\} C_{24}[H^\pm A^0 h^0] \\
&+ \left\{ K(\alpha,\beta) m_{H^0}^2 + J(\alpha,\beta)(-m_{H^0}^2 + 2m_{H^\pm}^2) - \frac{\sin(\alpha+\beta)}{\sin\beta\cos\beta} m_3^2 \right\} \cos 2\theta_W C_{24}[H^0 H^\pm H^\pm] \\
&+ \left\{ L(\alpha,\beta) m_{h^0}^2 - J(\alpha,\beta)(-m_{h^0}^2 + 2m_{H^\pm}^2) - \frac{\cos(\alpha+\beta)}{\sin\beta\cos\beta} m_3^2 \right\} \cos 2\theta_W C_{24}[h^0 H^\pm H^\pm] \\
&+ J(\alpha,\beta)(m_{H^\pm}^2 - m_{H^0}^2) C_{24}[w^\pm z^0 H^0] - J(\alpha,\beta)(m_{H^\pm}^2 - m_{h^0}^2) C_{24}[w^\pm z^0 h^0] \\
&- J(\alpha,\beta)(m_{H^\pm}^2 - m_{H^0}^2) \cos 2\theta_W C_{24}[H^0 w^\pm w^\pm] \\
&+ J(\alpha,\beta)(m_{H^\pm}^2 - m_{h^0}^2) \cos 2\theta_W C_{24}[h^0 w^\pm w^\pm] \\
&- J(\alpha,\beta)(m_{H^\pm}^2 - m_{A^0}^2) \left(C_{24}[w^\pm H^0 A^0] - C_{24}[w^\pm h^0 A^0] \right) \\
&- J(\alpha,\beta) m_W^2 \left(C_{24}[W^\pm H^0 A^0] - C_{24}[W^\pm h^0 A^0] \right)
\end{aligned}$$

$$
\begin{aligned}
&+J(\alpha,\beta)\frac{\cos 2\theta_W}{\cos\theta_W}m_W^2 C_{24}[H^\pm H^0 Z^0] - J(\alpha,\beta)\frac{\cos 2\theta_W}{\cos\theta_W}m_W^2 C_{24}[H^\pm h^0 Z^0] \\
&-J(\alpha,\beta)m_W^2\left\{4(m_W^2+p_W\cdot p_Z)C_0 + 2(2p_W+p_Z)\cdot(p_W C_{11}+p_Z C_{12})\right. \\
&\qquad\left.+p_W\cdot p_Z C_{23}+4C_{24}\right\}[W^\pm Z^0 H^0] \\
&+J(\alpha,\beta)m_W^2\left\{4(m_W^2+p_W\cdot p_Z)C_0 + 2(2p_W+p_Z)\cdot(p_W C_{11}+p_Z C_{12})\right. \\
&\qquad\left.+p_W\cdot p_Z C_{23}+4C_{24}\right\}[W^\pm Z^0 h^0] \\
&+J(\alpha,\beta)\cos^2\theta_W m_W^2\left\{(m_Z^2-m_W^2)C_0 - 2p_Z\cdot(p_W C_{11}+p_Z C_{12})\right. \\
&\qquad\left.+p_W\cdot p_Z C_{23}+4C_{24}\right\}[H^0 W^\pm W^\pm] \\
&-J(\alpha,\beta)\cos^2\theta_W m_W^2\left\{(m_Z^2-m_W^2)C_0 - 2p_Z\cdot(p_W C_{11}+p_Z C_{12})\right. \\
&\qquad\left.+p_W\cdot p_Z C_{23}+4C_{24}\right\}[h^0 W^\pm W^\pm] \\
&-J(\alpha,\beta)m_Z^2(m_{H^\pm}^2-m_{H^0}^2)\sin^2\theta_W C_0[w^\pm Z^0 H^0] \\
&+J(\alpha,\beta)m_Z^2(m_{H^\pm}^2-m_{h^0}^2)\sin^2\theta_W C_0[w^\pm Z^0 h^0] \\
&-J(\alpha,\beta)m_W^2(m_{H^\pm}^2-m_{H^0}^2)\sin^2\theta_W C_0[H^0 W^\pm w^\pm] \\
&+J(\alpha,\beta)m_W^2(m_{H^\pm}^2-m_{h^0}^2)\sin^2\theta_W C_0[h^0 W^\pm w^\pm] \\
&+J(\alpha,\beta)m_W^2\sin^2\theta_W\left(C_{24}[H^0 w^\pm W^\pm] - C_{24}[h^0 w^\pm W^\pm]\right)\Big], \qquad \text{(A.2)}
\end{aligned}
$$

where m_3 is defined as $m_3^2 = \mu_3^2/\sin\beta\cos\beta$.

$$
\begin{aligned}
&F^{(\mathrm{b})} = \frac{2}{16\pi^2 v^2\cos\theta_W} \\
&\times\left[-\frac{1}{2}\left\{K(\alpha,\beta)m_{H^0}^2 + J(\alpha,\beta)(-m_{H^0}^2+2m_{H^\pm}^2) - \frac{\sin(\alpha+\beta)}{\sin\beta\cos\beta}m_3^2\right\}\sin^2\theta_W B_0[H^0 H^\pm]\right. \\
&-\frac{1}{2}\left\{L(\alpha,\beta)m_{h^0}^2 - J(\alpha,\beta)(-m_{h^0}^2+2m_{H^\pm}^2) - \frac{\cos(\alpha+\beta)}{\sin\beta\cos\beta}m_3^2\right\}\sin^2\theta_W B_0[h^0 H^\pm] \\
&-\frac{1}{2}J(\alpha,\beta)(m_{H^\pm}^2-m_{H^0}^2)\sin^2\theta_W B_0[H^0 w^\pm] + \frac{1}{2}J(\alpha,\beta)(m_{H^\pm}^2-m_{h^0}^2)\sin^2\theta_W B_0[h^0 w^\pm] \\
&+J(\alpha,\beta)m_W^2\sin^2\theta_W\left(B_0[p_W;W^\pm H^0] - B_0[p_W;W^\pm h^0]\right) \\
&+J(\alpha,\beta)m_Z^2\sin^2\theta_W\left(B_0[p_Z;Z^0 H^0] - B_0[p_Z;Z^0 h^0]\right) \\
&+\frac{1}{2}\left\{K(\alpha,\beta)m_{H^0}^2 + J(\alpha,\beta)(-m_{H^0}^2+2m_{H^\pm}^2) - \frac{\sin(\alpha+\beta)}{\sin\beta\cos\beta}m_3^2\right\}\frac{m_{H^0}^2-m_{H^\pm}^2}{p^2-m_W^2}\sin^2\theta_W B_0[H^0 H^\pm] \\
&+\frac{1}{2}\left\{L(\alpha,\beta)m_{h^0}^2 - J(\alpha,\beta)(-m_{h^0}^2+2m_{H^\pm}^2) - \frac{\cos(\alpha+\beta)}{\sin\beta\cos\beta}m_3^2\right\}\frac{m_{h^0}^2-m_{H^\pm}^2}{p^2-m_W^2}\sin^2\theta_W B_0[h^0 H^\pm] \\
&+\frac{1}{2}J(\alpha,\beta)m_{H^0}^2\frac{m_{H^0}^2-m_{H^\pm}^2}{p^2-m_W^2}\sin^2\theta_W B_0[H^0 w^\pm]
\end{aligned}
$$

$$
\begin{aligned}
&-\frac{1}{2}J(\alpha,\beta)m_{h^0}^2\frac{m_{h^0}^2-m_{H^\pm}^2}{p^2-m_W^2}\sin^2\theta_W B_0[h^0w^\pm]\\
&+\frac{1}{2}\left\{K(\alpha,\beta)m_{H^0}^2+J(\alpha,\beta)(-m_{H^0}^2+2m_{H^\pm}^2)-\frac{\sin(\alpha+\beta)}{\sin\beta\cos\beta}m_3^2\right\}\\
&\qquad\times\frac{m_W^2}{p^2-m_W^2}\sin^2\theta_W(B_0+2B_1)[H^0H^\pm]\\
&+\frac{1}{2}\left\{L(\alpha,\beta)m_{h^0}^2-J(\alpha,\beta)(-m_{h^0}^2+2m_{H^\pm}^2)-\frac{\cos(\alpha+\beta)}{\sin\beta\cos\beta}m_3^2\right\}\\
&\qquad\times\frac{m_W^2}{p^2-m_W^2}\sin^2\theta_W(B_0+2B_1)[h^0H^\pm]\\
&+J(\alpha,\beta)m_W^4\frac{1}{p^2-m_W^2}\sin^2\theta_W(B_0-B_1)[H^0W^\pm]\\
&-J(\alpha,\beta)m_W^4\frac{1}{p^2-m_W^2}\sin^2\theta_W(B_0-B_1)[h^0W^\pm]\\
&+J(\alpha,\beta)m_W^2\frac{m_{H^0}^2-m_{H^\pm}^2}{p^2-m_W^2}\sin\theta_W(B_0+2B_1)[H^0w^\pm]\\
&-J(\alpha,\beta)m_W^2\frac{m_{H^0}^2-m_{H^\pm}^2}{p^2-m_W^2}\sin^2\theta_W(B_0+2B_1)[h^0w^\pm]\Bigg].
\end{aligned}
\tag{A.3}
$$

$$
\begin{aligned}
F^{(\mathrm{c})} &= \frac{2}{16\pi^2v^2\cos\theta_W}\\
&\times\left(\frac{1}{2}\Bigg[\ \tilde{\Pi}^{(2)}_{H^\pm w^\mp}\times\frac{1}{p^2-m_W^2}\sin^2\theta_W\right.\\
&\quad-\sin^2\theta_W\left\{\sin(\alpha-\beta)\frac{1}{m_{H^0}^2}\tilde{T}_H+\cos(\alpha-\beta)\frac{1}{m_{h^0}^2}\tilde{T}_h\right\}\\
&\quad+\sin^2\theta_W\frac{m_{H^\pm}^2}{p^2-m_W^2}\left\{\sin(\alpha-\beta)\frac{1}{m_{H^0}^2}\tilde{T}_H+\cos(\alpha-\beta)\frac{1}{m_{h^0}^2}\tilde{T}_h\right\}\\
&\quad-\sin^2\theta_W\frac{1}{p^2-m_W^2}\left\{\sin(\alpha-\beta)\tilde{T}_H+\cos(\alpha-\beta)\tilde{T}_h\right\}\\
&\quad-\left.\sin^2\theta_W\frac{m_W^2}{p^2-m_W^2}\left\{\sin(\alpha-\beta)\frac{1}{m_{H^0}^2}\tilde{T}_H+\cos(\alpha-\beta)\frac{1}{m_{h^0}^2}\tilde{T}_h\right\}\Bigg]\right)\\
&= \frac{\sin^2\theta_W}{16m_{H^\pm}^2v^2\cos\theta_W}\frac{1}{p^2-m_W^2}\\
&\times\left[\left\{K(\alpha,\beta)m_{H^0}^2-2J(\alpha,\beta)m_{H^0}^2-\frac{\sin(\alpha+\beta)}{\sin\beta\cos\beta}m_3^2\right\}A(m_{H^\pm}^2)\right.\\
&\quad+\left\{L(\alpha,\beta)m_{h^0}^2+2J(\alpha,\beta)m_{h^0}^2-\frac{\cos(\alpha+\beta)}{\sin\beta\cos\beta}m_3^2\right\}A(m_{H^\pm}^2)\\
&\quad-\left\{K(\alpha,\beta)m_{H^0}^2-\frac{\sin(\alpha+\beta)}{\sin\beta\cos\beta}m_3^2\right\}A(m_{H^0}^2)
\end{aligned}
$$

$$- \left\{ L(\alpha,\beta) m_{h^0}^2 - \frac{\cos(\alpha+\beta)}{\sin\beta\cos\beta} m_3^2 \right\} A(m_{h^0}^2) + J(\alpha,\beta)(m_{H^0}^2 - m_{h^0}^2) A(m_W^2) \Bigg], \quad \text{(A.4)}$$

where $\tilde{T}_H$ and $\tilde{T}_h$ are the tadpole graphs factorized by $1/(16\pi^2 v^3)$. $\tilde{\Pi}^{(2)}_{H^\pm w^m p}$ is the $1/(16\pi^2 v^2)$-factorized contribution of the two-point function which can be written in terms of the A-function. The full expressions for these are given in Eqs (A.7), (A.8) and (A.9).

$$\begin{aligned}
G^{(\mathrm{a})} &= \frac{2m_W^2}{16\pi^2 v^2 \cos\theta_W} \\
&\times \Bigg[- \left\{ K(\alpha,\beta) m_{H^0}^2 + J(\alpha,\beta)(-m_{H^0}^2 + 2m_{H^\pm}^2) - \frac{\sin(\alpha+\beta)}{\sin\beta\cos\beta} m_3^2 \right\} (C_{12}+C_{23}) [H^\pm A^0 H^0] \\
&- \left\{ L(\alpha,\beta) m_{h^0}^2 - J(\alpha,\beta)(-m_{h^0}^2 + 2m_{H^\pm}^2) - \frac{\cos(\alpha+\beta)}{\sin\beta\cos\beta} m_3^2 \right\} (C_{12}+C_{23}) [H^\pm A^0 h^0] \\
&+ \left\{ K(\alpha,\beta) m_{H^0}^2 + J(\alpha,\beta)(-m_{H^0}^2 + 2m_{H^\pm}^2) - \frac{\sin(\alpha+\beta)}{\sin\beta\cos\beta} m_3^2 \right\} \cos 2\theta_W (C_{12}+C_{23}) [H^0 H^\pm H^\pm] \\
&+ \left\{ L(\alpha,\beta) m_{h^0}^2 - J(\alpha,\beta)(-m_{h^0}^2 + 2m_{H^\pm}^2) - \frac{\cos(\alpha+\beta)}{\sin\beta\cos\beta} m_3^2 \right\} \cos 2\theta_W (C_{12}+C_{23}) [h^0 H^\pm H^\pm] \\
&+ J(\alpha,\beta)(m_{H^\pm}^2 - m_{H^0}^2)(C_{12}+C_{23}) [w^\pm z^0 H^0] \\
&- J(\alpha,\beta)(m_{H^\pm}^2 - m_{h^0}^2)(C_{12}+C_{23}) [w^\pm z^0 h^0] \\
&- J(\alpha,\beta)(m_{H^\pm}^2 - m_{H^0}^2) \cos 2\theta_W (C_{12}+C_{23}) [H^0 w^\pm w^\pm] \\
&+ J(\alpha,\beta)(m_{H^\pm}^2 - m_{h^0}^2) \cos 2\theta_W (C_{12}+C_{23}) [h^0 w^\pm w^\pm] \\
&- J(\alpha,\beta)(m_{H^\pm}^2 - m_{A^0}^2) \left\{ (C_{12}+C_{23}) [w^\pm H^0 A^0] - (C_{12}+C_{23}) [w^\pm h^0 A^0] \right\} \\
&- J(\alpha,\beta) m_W^2 \left(2C_0 + 2C_{11} + C_{12} + C_{23}\right) [W^\pm H^0 A^0] \\
&+ J(\alpha,\beta) m_W^2 \left(2C_0 + 2C_{11} + C_{12} + C_{23}\right) [W^\pm h^0 A^0] \\
&- J(\alpha,\beta) \frac{\cos 2\theta_W}{\cos\theta_W} m_W^2 (-C_{12} + C_{23}) [H^\pm H^0 Z^0] \\
&+ J(\alpha,\beta) \frac{\cos 2\theta_W}{\cos\theta_W} m_W^2 (-C_{12} + C_{23}) [H^\pm h^0 Z^0] \\
&+ J(\alpha,\beta) m_W^2 \left(2C_0 - 2C_{11} + 5C_{12} + C_{23}\right) [W^\pm Z^0 H^0] \\
&- J(\alpha,\beta) m_W^2 \left(2C_0 - 2C_{11} + 5C_{12} + C_{23}\right) [W^\pm Z^0 h^0] \\
&+ J(\alpha,\beta) \cos^2\theta_W m_W^2 \left(4C_{11} - 3C_{12} - C_{23}\right) [H^0 W^\pm W^\pm] \\
&- J(\alpha,\beta) \cos^2\theta_W m_W^2 \left(4C_{11} - 3C_{12} - C_{23}\right) [h^0 W^\pm W^\pm] \\
&+ J(\alpha,\beta) m_W^2 \sin^2\theta_W \left\{ (C_{23} - C_{12}) [H^0 w^\pm W^\pm] - (C_{23} - C_{12}) [h^0 w^\pm W^\pm] \right\} \Bigg]. \qquad \text{(A.5)}
\end{aligned}$$

$$G^{(\mathrm{b})} = G^{(\mathrm{c})} = H^{(\mathrm{a,b\ and\ c})} = 0. \qquad \text{(A.6)}$$

The tadpole graphs $T_H(=\tilde{T}_H/(16\pi^2v^3))$ and $T_h(=\tilde{T}_h/(16\pi^2v^3))$ are calculated as

$$
\begin{aligned}
T_H &= \frac{1}{16\pi^2v^3}\left[m_{H^0}^2\cos(\alpha-\beta)\left(A[w^\pm]+\frac{1}{2}A[z^0]\right)\right.\\
&+\left\{m_{H^0}^2\left(\frac{\cos\alpha\sin^2\beta}{\cos\beta}-\frac{\sin\alpha\cos^2\beta}{\sin\beta}\right)+2m_{H^\pm}^2\cos(\alpha-\beta)+\frac{\sin(\alpha+\beta)}{\sin\beta\cos\beta}m_3^2\right\}A[H^\pm]\\
&+\left\{m_{H^0}^2\left(\frac{\cos\alpha\sin^2\beta}{\cos\beta}-\frac{\sin\alpha\cos^2\beta}{\sin\beta}\right)+2m_{A^0}^2\cos(\alpha-\beta)-\frac{\sin(\alpha+\beta)}{\sin\beta\cos\beta}m_3^2\right\}\frac{A[A^0]}{2}\\
&+\frac{3}{2}\left\{\left(\frac{\cos^3\alpha}{\cos\beta}+\frac{\sin^3\alpha}{\sin\beta}\right)m_{H^0}^2-\frac{\cos2\beta}{\cos\beta\sin\beta}\sin(\alpha-\beta)m_3^2\right\}A[H^0]\\
&+\left\{\frac{1}{2}(m_{H^0}^2+2m_{h^0}^2)\frac{\sin2\alpha}{\sin2\beta}-\frac{m_3^2}{4\cos\beta\sin\beta}(-3\sin2\alpha+\sin2\beta)\right\}\cos(\alpha-\beta)A[h^0]\\
&\left.+8\cos(\alpha-\beta)\left(m_W^2A[W^\pm]+\frac{1}{2}m_Z^2A[Z^0]\right)\right], \qquad \text{(A.7)}\\
T_h &= \frac{1}{16\pi^2v^3}\left[-m_{h^0}^2\sin(\alpha-\beta)\left(A[w^\pm]+\frac{1}{2}A[z^0]\right)\right.\\
&+\left\{m_{h^0}^2\left(\frac{\sin\alpha\sin^2\beta}{\cos\beta}-\frac{\cos\alpha\cos^2\beta}{\sin\beta}\right)-2m_{H^\pm}^2\sin(\alpha-\beta)+\frac{\cos(\alpha+\beta)}{\sin\beta\cos\beta}m_3^2\right\}A[H^\pm]\\
&+\left\{m_{h^0}^2\left(\frac{\sin\alpha\sin^2\beta}{\cos\beta}-\frac{\cos\alpha\cos^2\beta}{\sin\beta}\right)-2m_{A^0}^2\sin(\alpha-\beta)+\frac{\cos(\alpha+\beta)}{\sin\beta\cos\beta}m_3^2\right\}\frac{A[A^0]}{2}\\
&-\frac{3}{2}\left\{\left(\frac{\sin^3\alpha}{\cos\beta}-\frac{\cos^3\alpha}{\sin\beta}\right)m_{h^0}^2+\frac{\cos2\beta}{\cos\beta\sin\beta}\cos(\alpha-\beta)m_3^2\right\}A[h^0]\\
&+\frac{1}{2}\left\{(2m_{H^0}^2+m_{h^0}^2)\frac{\sin2\alpha}{\sin2\beta}-\frac{m_3^2}{4\cos\beta\sin\beta}(3\sin2\alpha+\sin2\beta)\right\}\sin(\alpha-\beta)A[H^0]\\
&\left.-8\sin(\alpha-\beta)\left(m_W^2A[W^\pm]+\frac{1}{2}m_Z^2A[Z^0]\right)\right]. \qquad \text{(A.8)}
\end{aligned}
$$

Finally, $\Pi_{H^\pm w^\mp}(=\tilde{\Pi}_{H^\pm w^\mp}/(16\pi^2v^2))$ is given by

$$
\begin{aligned}
\Pi_{H^\pm w^\mp}^{(2)} &= \frac{1}{16\pi^2v^2}\left[2(m_{H^0}^2-m_{h^0}^2)J(\alpha,\beta)\left(A[W^\pm]+\frac{1}{4}A[Z^0]\right)\right.\\
&+2\left\{K(\alpha,\beta)-J(\alpha,\beta)-\frac{\sin(\alpha+\beta)}{\sin\beta\cos\beta}m_3^2\right\}m_{H^0}^2A[H^\pm]\\
&+2\left\{L(\alpha,\beta)+J(\alpha,\beta)-\frac{\cos(\alpha+\beta)}{\sin\beta\cos\beta}m_3^2\right\}m_{h^0}^2A[H^\pm]\\
&+\frac{1}{4}\left\{\sin2\beta\left(\frac{\sin^2\alpha}{\sin^2\beta}-\frac{\cos^2\alpha}{\cos^2\beta}\right)-\sin2(\alpha-\beta)\right\}m_{H^0}^2A[A^0]\\
&+\frac{1}{4}\left\{\sin2\beta\left(\frac{\cos^2\alpha}{\sin^2\beta}-\frac{\sin^2\alpha}{\cos^2\beta}\right)+\sin2(\alpha-\beta)\right\}m_{h^0}^2A[A^0]\\
&-\cot2\beta\,m_3^2\,A[A^0]\\
&\left.+\frac{1}{4}\sin2\beta\left(\frac{\sin^4\alpha}{\sin^2\beta}-\frac{\cos^4\alpha}{\cos^2\beta}+\frac{\sin2\alpha\cos2\alpha}{\sin2\beta}\right)m_{H^0}^2A[H^0]\right.
\end{aligned}
$$

$$
\begin{aligned}
&+\frac{1}{4}\sin 2\beta\left(\frac{\sin^2\alpha\cos^2\alpha}{\sin^2\beta}-\frac{\sin^2\alpha\cos^2\alpha}{\cos^2\beta}-\frac{\sin 2\alpha\cos 2\alpha}{\sin 2\beta}\right)m_{h^0}^2A[H^0]\\
&-\frac{m_3^2}{2}\frac{\cos 2\beta}{\cos\beta\sin\beta}\left(\sin^2(\alpha-\beta)A[H^0]+\cos^2(\alpha-\beta)A[h^0]\right)\\
&+J(\alpha,\beta)m_{H^\pm}^2\left(A[h^0]-A[H^0]\right)\\
&+\frac{1}{4}\sin 2\beta\left(\frac{\sin^2\alpha\cos^2\alpha}{\sin^2\beta}-\frac{\cos^2\alpha\sin^2\alpha}{\cos^2\beta}-\frac{\sin 2\alpha}{\sin 2\beta}\cos 2\alpha\right)m_{H^0}^2A[h^0]\\
&+\frac{1}{4}\sin 2\beta\left(\frac{\cos^4\alpha}{\sin^2\alpha}-\frac{\sin^4\alpha}{\cos^2\beta}+\frac{\sin 2\alpha\cos 2\alpha}{\sin 2\beta}\right)m_{h^0}^2A[h^0]\Big]. \qquad \text{(A.9)}
\end{aligned}
$$

APPENDIX 2: Calculation of $H^+ \to W_L^+ Z_L^0$ by the use of the equivalence theorem

As shown in Sec 4-1, at large $m_{H^\pm}$ region, the longitudinally polarized final gauge bosons become the dominant mode in $H^+ \to W^+Z^0$. In such case, we can check the results of the full calculation by the use of the equivalence theorem [30, 31], which says that $\Gamma(H^+ \to W_L^+ Z_L^0) \sim \Gamma(H^+ \to w^+ z^0)$ for $m_{H^\pm} \gg m_W$. The much simpler calculation of $\Gamma(H^+ \to w^+ z^0)$ can be useful to check the consistency of the full calculation. Here we show the explicit results of the amplitude $\mathcal{M}_{ET}(H^+ \to w^+ z^0)$ calculated in the Landau gauge (See Fig 3.). We can clearly see in Eq (A.10) that $\mathcal{M}_{ET} \sim 0$ for $m_{H_\pm} \sim m_{A^0}$.

$$
\begin{aligned}
&\mathcal{M}_{ET}(H^+ \to w^+ z^0) = \frac{i}{v^3}(m_{H^\pm}^2 - m_{A^0}^2)\\
&\times\Big[\Big\{K(\alpha,\beta)m_{H^0}^2 - J(\alpha,\beta)(m_{H^0}^2 - 2m_{H^\pm}^2)\Big\}(m_{H^0}^2 - m_{A^0}^2)C_0[H^\pm, A^0, H^0]\\
&\quad+\Big\{L(\alpha,\beta) + J(\alpha,\beta)(m_{h^0}^2 - 2m_{H^\pm}^2)\Big\}(m_{H^0}^2 - m_{A^0}^2)C_0[H^\pm, A^0, h^0]\\
&\quad+J(\alpha,\beta)m_{H^0}^2(m_{H^0}^2 - m_{A^0}^2)C_0[w^\pm, A^0, H^0]\\
&\quad-J(\alpha,\beta)m_{h^0}^2(m_{h^0}^2 - m_{A^0}^2)C_0[w^\pm, A^0, h^0]\\
&\quad-\Big\{K(\alpha,\beta)m_{H^0}^2 - J(\alpha,\beta)(m_{H^0}^2 - 2m_{H^\pm}^2)\Big\}B_0[H^0, H^\pm]\\
&\quad-\Big\{L(\alpha,\beta)m_{h^0}^2 + J(\alpha,\beta)(m_{h^0}^2 - 2m_{H^\pm}^2)\Big\}B_0[h^0, H^\pm]\\
&\quad+J(\alpha,\beta)(m_{H^0}^2 - m_{h^0}^2)B_0[A^0, w^\pm]\\
&\quad+\Big\{J(\alpha,\beta)(m_{h^0}^2 - m_{H^0}^2) + K(\alpha,\beta)m_{H^0}^2 - L(\alpha,\beta)m_{h^0}^2\Big\}B_0[0; H^\pm, A^0]\\
&\quad+J(\alpha,\beta)\Big\{m_{h^0}^2B_0[0; h^0, w^\pm] + m_{h^0}^2B_0[0; h^0, z^0] - m_{H^0}^2B_0[0; H^0, w^\pm]\\
&-m_{H^0}^2B_0[0; h^0, z^0] + (m_{H^0}^2 - m_{A^0}^2)C_0[0; H^0, A^0] - (m_{h^0}^2 - m_{A^0}^2)B_0[0; h^0, A^0]\Big\}\Big]. \qquad \text{(A.10)}
\end{aligned}
$$

References

[1] The LEP Collaborations, ALEPH, DELPHI, L3, OPAL, the LEP Electroweak Working Group and the SLD Heavy Flavour Group, preprint CERN-PRE/96-183.

[2] K. Hagiwara, S. Matsumoto, and D. Haidt, Preprint KEK-TH-512, KEK Preprint 97-86, DESY 96-192, `hep-ph/9706331`; K. Hagiwara, S. Matsumoto, D. Haidt and C.S. Kim, Z. Phys. **C64**, 559 (1994).

[3] A.Ballestrero *et. al.*, *Proceedings of the Workshop on Physics at LEP2*, G. Altarelli, T. Sjöstrand and F. Zwirner (eds.), CERN Yellow Report CERN 96-01 (1996).

[4] CMS Thechnical Proposal, CERN/LHCC/94-38,
ATRAS Thechnical Proposal, CERN/LHCC/94-38.

[5] *Physics and Technology of the Next Linear Collider: a Report submitted to Snowmass 1996,* BNL 52-502, FNAL-PUB-96/112, LBNL-PUB-5425, SLAC Report 485, UCRL-ID-124160; *JLC-1,*KEK Report 92-16 (1992).

[6] J.F. Gunion, H.E. Haber, G. Kane and S. Dawson, *The Higgs Hunter's Guide*, (Addison-Wesley, New York, 1990).

[7] M.S. Alam et al. Phys. Rev. Let. **74**, 2885 (1995).

[8] T. Goto and Y. Okada, Prog. Theor. Phys. **94**, 407 (1995).

[9] J.A. Grifols and A. Méndez, Phys. Rev. D **22**, 1725 (1980).

[10] A. Méndez and A. Pomarol, Nucl. Phys. **B349**, 369 (1991).

[11] M. Capdequi Peyranère, H.E. Haber and P. Irulegui, Phys. Rev. D **44**, 191 (1991).

[12] CDF Collaboration, F. Abe *et al.*, Phys. Rev. Lett. **73**, 225 (1994).

[13] T. Inami, T. Kawakami, and C.S. Lim, Mod. Phys. Lett. **A 10**, 1471 (1995).

[14] R.M. Godbole, B. Mukhopadhyaya and M. Nowakowski, Phys. Lett. **B352** 388 (1995).

[15] T.G. Rizzo, Mod. Phys. Lett. **A 4**, 2757 (1989).

[16] T. Appelquist and J. Carrazone, Phys. Rev. D **11**, 2856 (1975).

[17] T. Appelquist and C. Bernard, Phys.Rev. D **22**, 200 (1980).

[18] P. Ciafaloni and D. Esprin, Preprint UAB-FT-405, UB-ECM-PF-96/23, (`hep-ph/9612383`).

[19] S. Kanemura and H-A. Tohyama, KEK Preprint 97-96, KEK-TH-528, OU-HET 271, (`hep-ph/9707454`).

[20] M. Veltman, Acta. Phys. Pol. **B 8**, 475 (1977), Phys. Lett. **70 B**, 253 (1977); M. Einhorn and J. Wudka, Phys. Rev. D **39**, 2758 (1989), *ibid.* **47** 5029 (1993).

[21] H.E. Haber and A. Pomarol, Phys. Lett. **B302**, 435 (1993).

[22] S. Kanemura, T. Kubota, and H-A. Tohyama, Nucl. Phys. **B483**, 111 (1997).

[23] A.K. Grant, Phys. Rev. D **51**, 207 (1995).

[24] S. Kanemura, T. Kubota and E. Takasugi, Phys. Lett. **B313**, 155 (1993).

[25] J.F. Gunion, G.L. Kane, and J. Wudka, Nucl. Phys. **B299**, 231 (1988).

[26] S. Glashow and S. Weinberg, Phys. Rev. D **15**, 1958 (1977).

[27] S. Weinberg, Phys. Rev. D **42**, 860 (1990).

[28] S. Weinberg, Phys. Rev. D **19**, 1277 (1979); L. Susskind, *ibid.* **20**, 2619 (1979).

[29] H. Georgi, Hadir. J. Phys. **1**, 155 (1978).

[30] J.M. Cornwall, D.N. Levin, and G. Tiktopoulos, Phys. Rev. D **10**, 1145 (1974); B.W. Lee, C. Quigg, and H.B. Thacker, *ibid.* **16**, 1519 (1977).

[31] M.S. Chanowitz and M.K. Gaillard, Nucl. Phys. **B261**, 379 (1985); H-J. He, Y-P. Kuang and X. Li, Phys. Rev. D **49**, 4842 (1994), and references therein.

[32] J. Hisano, S. Kiyoura, and H. Murayama, Phys. Lett.**B399**, 156 (1997).

[33] V.Barger, J.L.Hewett and R.J.N.Phillips, Phys. Rev. D **41**, 3432 (1990); A.J. Buras, P. Krawczyk, M.E. Lautenbacher, and C. Salazar, Nucl. Phys. **B337**, 284 (1990).

[34] J. Preskill, S.P. Trivedi, and F. Wilczek, Nucl. Phys. **B363**, 207 (1991).

[35] T.G. Rizzo, Phys. Rev. D **39**, 728 (1989).

[36] R.M. Barnett, H.E. Haber, and D.E. Soper, Nucl. Phys. **B306**, 697 (1988).

[37] G. Passarino and M. Veltman, Nucl. Phys. **B160**, 151 (1979).